Symbol Synchronizer Assembly Instability Study

R. C. Bunce
Network Operations Office

This first part of a two-part analysis describes the unstable operation of the Symbol Synchronizer Assembly (SSA) in the narrow-narrow configuration at 8⅓ bits/s. Reduction of a data set signal-to-noise (dB) vs. time indicates that the SSA is cycling between unstable lock conditions and entirely out-of-lock or ramp conditions. The ramp condition is so called because a strong second-order frequency term or linear drift becomes obvious. The drift magnitude is far beyond loop tracking capability and even marginal when a data rate of 33⅓ bits/s is used. The data indicates a possible third-order term, noted casually in other unprocessed sets. Based on the ramp magnitude, it is finally recommended that bandwidths less than 0.01 Hz (design point) be avoided. Also, an outline is given of Part II, which extends the study to analyze the third-order possibility and will upgrade early results through sophisticated machine programming of statistical and iterative manipulations.

I. Introduction

The DSN Station symbol synchronizor assembly (SSA) performs according to design under all normally recommended operating conditions. However, the equipment contains operationally programmable configurations, outside of the recommended states, that result in unstable behavior.

Specifically, the predominant configuration leading to instability occurs when the narrowest bandwidth instruction (narrow-narrow) is combined with the lowest normally operational symbol rate (8⅓ bits/s). An increase in either the bandwidth instruction (to narrow-medium) or use of a higher symbol rate (nominal 33⅓ bits/s) usually relieves the instability.

Causes of the instability are not well understood. The stable operational threshold with respect to both bandwidth configuration and the product with input symbol rate is presently undefined.

The purpose of this analysis is to determine the magnitude of the instability parameters (by data reduction, particularly, raw points of signal-to-noise vs time), and, based on this analysis, state quantitative expressions that define the minimum stable SSA operating conditions, finally translated to a stable range of input instructions.

The analysis is in two parts. Part One develops elementary models of the unstable conditions and uses these to reduce a single data set to arrive at a preliminary second-order estimate of one of the parameters causing the unstable behavior and its effect on stable operational minimums. Approximate expressions are used to form the preliminary model.

Part Two, now being performed will generalize the reduction of a number of data sets, exhibiting various modes of instability to third order (prelock and lock, periodic, divergent) to bound the extent of the casual parameters and their source. More sophisticated expressions (particularly the relation between signal-to-noise in decibels and integrated phase processes) will be used, and best-estimate minimal stable operational conditions, statistically bounded, will be recommended.

II. SSA Data and Modes

This discussion will be limited to a single data set taken at CTA 21 in February, using the "narrow-narrow" 8⅓ bps condition, within which the instability is most pronounced. This unstable behavior is apparently not directly related to input signal-to-noise ratio, measured in decibels (S/N), but rather due to independent internal effects. When S/N is large, the instability effect remains unchanged.[1] The SSA acts nominally as a normal second-order phase-lock-loop.

Initial thoughts were that the instability was simple oscillator low-frequency $1/f$ noise, and could be treated as such; this noise form is common with very narrow phase-lock-loops, independent of input S/N, and in narrow-narrow, 8⅓ condition, the SSA design loop bandwidth is only 0.00125 Hz.

Data Set No. 1, S/N vs time, plotted in Fig. 1, is typical. Data was taken with straight square-wave input signals at S/N of about 17 dB. It is immediately apparent that the data is not random, but *deterministic*, except for obvious minor first-order noise effects. It can be fit (piecewise) to some kind of deterministic model or curve set, except possibly around the null points. This does not mean that the data is not statistical in the long run; whatever is causing the variations (probably temperature effects on local oscillators) may change state, or otherwise vary randomly at large intervals. The question is philosophical; the given data set, observed over a relatively short time period (with respect to bandwidth reciprocal) shows a deterministic trend or pattern. Low-frequency noise statistics must be abandoned; we are observing effects from a single, causal, and directly determinable time-dependent source.

The most informative feature in Fig. 1 is the presence of nulls. The SSA S/N measurement set is obtained by integrating across sequential symbol periods and summing results; a null could happen only if transitions occurred near the half-way point through a symbol period, a phase error of ¼ cycle, or 90 deg. This is well outside the SSA loop control range. The instability is an "in-loop-control"—"out-of-loop-control" phenomenon.[2] The control range (the phase-detector integral) is only ± 1/16 cycle, or ± 22.5 deg.

The 22.5 deg range leads immediately to another conclusion: if the actual input S/N is stable and has a peak value at 0 deg, and if the S/N (average) drops by 2.48 dB, loop control is lost. This is somewhat distorted by S/N summation effects; but, in general, the loop is not fully active if the S/N is less than 2.48 dB below peak. The figure is simply the loop S/N mean integrator output at ± 22.5 deg or 1/16 cycle, from zero phase error.

It is, therefore, obvious that the disturbing force under the stated conditions is sufficient that the loop cannot hold control; i.e., maintain lock. The most causal parameter to do this in a second-order-loop is a *frequency ramp* with magnitude beyond the tracking range. Although various spotty but observed data sets, including Set No. 1, have shown possible higher-order components, Data Set No. 1 (even intuitively) shows a strong second-order parabolic curvature. Higher-order components of significance cause multiple nulls, or, at least, successive inflections. These are minor in Data Set No. 1. See Appendix for additional discussion.

The predominant question of Fig. 1 is whether or not the signal reentered loop control at the central peak. If it did not, then the frequency turned over, due to the frequency ramp, and reentered negatively following the next null. If it did reenter, then the S/N must have been variable, with a peak of only 14 dB in the central region, or data points at the peak were missed. Consider

[1] S/N data amplitude follows the signal level, but the time-dependent form of the instability process does not change appreciably with this amplitude.

[2] Some would say "in-lock"—"out-of-lock". However, if lock is defined as a zero or steady-state phase error, the loop simply "has control" or "is out of control." When it can't "handle" the signal, it is never "in lock".

the first hypothesis above to be Mode I and the second Mode II. The S/N data cannot resolve this, for SSA S/N reduction is based on absolute values, and the sign of the error phase is indeterminate. This leads to the discussion of S/N as an indicator of phase.

III. SSA Signal-to-Noise (dB) to Phase Conversion

The SSA S/N readout results from processing of the summation of the absolute values (and their squares) of a set of measures obtained by integration over the symbol period. The result is simply the square of the mean measure (signal estimate, watts) over its variance (noise estimate, watts). It would be accurate, except that absoluting the measures causes a dc offset by noise, an inescapable error. The error becomes significant if the integrated signal component approaches the noise component. The measure then becomes nearly indeterminate; all outputs approximate 0 dB with little quantitative information possible. In general, when the SSA S/N readout is below 3 dB the number is indefinite and becomes nearly meaningless at about 1.0 dB. Detailed mathematics are omitted at this time, as the algorithm problems in the area are well known. It is handled here simply by disregarding one point of low S/N data; the point, at 0.4 dB, was obviously inaccurate. Under high S/N conditions, the S/N integral is directly proportional to the phase error across a single quadrant. The true signal level is measured at zero phase error, while the null occurs at ¼ cycle of phase error, or 90 deg, when the transition is at the integral mid-point and the two halves cancel. Thus, the elementary reduction of S/N to phase is

$$\hat{\phi}(t) = n \cdot \frac{1}{2} \pm \frac{1}{4}\left\{1 - 10\exp\left[-\left(\frac{DBX - DB(t)}{20}\right)\right]\right\} \tag{1}$$

where

$\hat{\phi}(t)$ = phase estimate with time-tag t.

DBX = system S/N, dB; the peak observed value.

$DB(t)$ = S/N readout at time t.

$n, \pm$ = index and sign choice to fix $\hat{\phi}$ according to selected mode estimate.

For data set No. 1, n, sign, and DBX were chosen as follows; see Figure 1 for null and peak position ($t = T$).

A plot of data set Number 1, both modes, and reduced to phase equivalents by Eq. (1) and Table 1, is shown in Fig. 2. This was the basic working data model for Part 1. Note uncertainty regions near nulls, and also the very narrow loop periods; the signal is out of loop control for the majority of the time. The most significant and unambiguous region is the long-ramp section between 400 and 600 s. Except for sign, this section is independent of mode, and was finally the prime data field used for analysis.

Since actual S/N readout is the result of summation over an S/N interval (30 s), Expression (1) can only be approximate. The actual phase representing a given readout is some median value within the summation, and occurs at some variable time in this period. However, without parameter estimates for the data model, corrections are impossible; in turn, parameter estimates depend on phase points. An iteration process is indicated, and a program for this is under way for use in Part II. Also, pure phase jitter, insignificant during loop periods, is not negligible in ramp periods, when loop feed-back does not control it. The program covering these effects is quite complicated, and its initial form was lost through computer malfunction before meaningful additional data sets could be obtained. However, Expression (1), with suitable initial correction near nulls for both the S/N algorithm and inherent phase jitter, was the first program step and is probably accurate within a few degrees, except near nulls.

Data Set No. 1, as reduced, showed, regardless of mode, an apparently fairly constant frequency during the out-of-loop-control, or ramp periods. However, an investigation of the data derivative, particularly in the indicated ramp period between 400 and 600 s, revealed an undeniable and relatively large second-order frequency term, or $\dot{F}$, and, (although the data was insufficient) even gave indications of a mild third-order process (to be disregarded at this time). Based on the strong ramp term, the hypothesis was established that the SSA voltage-controlled oscillator (VCO) (synthesizer sweep oscillator) was drifting. The Part I models for this internal ramp drift follow.

IV. SSA Phase-Lock Loop With Frequency Drift Models

The SSA is finally an ordinary second-order optimized loop with very narrow-band capability, and perfect integrator.

Under strong-signal input conditions (the only conditions of this study), the phase detector function (a combination of digital logic and analog-to-digital conversion of an integral) is linear over the range $\pm 1/16$ cycle, or ± 22.5 deg; a cycle period being two symbol periods.

When the phase error exceeds the above limits, the phase detector output becomes a nominal constant until the phase error has increased to a point very close to null, $\pm 1/4$ cycle (see Appendix for variations). The output is then indeterminate for a few degrees, emerging again as constant, but with reverse polarity; the loop turns over while passing through a null. Beyond 22.5 deg, the loop exercises no phase jitter control.[3]

Ordinarily, the detector null flip-flop condition would be a strong restoring force for loop lock. The VCO frequency differential reverses, and the ramp maximum component polarity reverses, driving the loop toward subsequent lock. Such $\dot{F}$ changes were not, however, discernible in the data, and it was concluded that they must be masked by the large internal source. However, for theoretical purposes, we include both in the models; under certain central conditions, the frequency-shift is significant and time-dependent.

A second-order phase-lock loop with internal drift has well known solutions; we assume the input signal to be a stable square-wave at phase zero.

The loop model with constant internal frequency drift, applying when the phase error is in control range, has the S-plane form:

$$\phi(s) = \frac{s\phi_0 - \dot{F}_0 - F_0/s}{(s+a)^2 + b^2} \tag{2}$$

ϕ_0 = initial phase error, cycles ($\pm 1/16$)

F_0 = initial frequency offset from center, Hz

$\dot{F}_0$ = (constant) drift rate, Hz/s

a, b = loop constants at operating point

Time solutions of Eq. (2) contain linear, exponential, and trigonometric terms, and vary with gain (a function of operating point). To simplify this initial part one study, data were taken in the region where parameter b is zero (unity damping); "a" is then ω_n or just "ω," nominally $4/3\ \omega_L \cdot \omega_L$ is the design bandwidth. The time solution for Eq. (2) is then free of trigonometric terms:

$$\phi(t)\big|_{b=0} = [(1-\omega t)e^{(-\omega t)}]\,\phi_0 - \frac{1}{\omega}[(\omega t)e^{(-\omega t)}]\,F_0 - \frac{1}{\omega^2}[1-(1-\omega t)e^{(-\omega t)}]\,\dot{F}_0 \tag{3a}$$

The ramp model is elementary; expressed as step functions:

$$\phi(t) = \phi_0' + (F_0 \pm \Delta F)\cdot t + (\dot{F}_0 \pm \Delta\dot{F})\cdot\frac{t^2}{2} \tag{3b}$$

$t = (T - T(\phi_0'))$: time "in the run"

$\Delta F = 2\omega\phi_L = \dfrac{\omega}{8}$

$\Delta\dot{F} = \phi_L \cdot \omega^2 = \omega^2/16$

$\pm$ = sign, as required for restoring lock.

Eq. (3b) was applied to the long-ramp data in Fig. 2, by least squares fit, and the frequency and rate constants were found to be in excess of F and $\dot{F}$ maximums, as expected. The loop model, Eq. (3a), was also applied, using the ramp results, to the few data points available. The errors were less than two degrees, but these loop results can obviously not be termed conclusive, for loop error variance was not within any kind of normal limits for the three points (25 deg). The ramp results are, however, significant, particularly when the indicated indefinite null point was omitted. Results follow.

V. Concluding Expressions

It is obvious why the SSA cannot hold lock—the internal drift is excessive in the narrowest bandwidth condition. In this condition, least squares fit under two conditions (using or omitting the final ramp point) were:

$$|\dot{F}| = [4 \cdot 132 \pm 0.68] \times 10^{-6}\ \text{Hz/s}$$

Phase error rms of the fits was only 0.69 deg, making the ± 0.68 approximately a one-sigma figure.

To track this requires:

$$\omega_{MIN} = [16 \times \dot{F}_{observed}]^{1/2} = 0.0081\ \text{Hz minimum} \tag{4}$$

At the 8⅓ bit/s rate, the bandwidth is 0.00167, well out of range. However, at a bit rate of 33⅓ bit/s, the equiva-

[3]Transitions, the time expression of phase, occur outside the phase detector gate, so their position cannot be included in loop feedback.

lent design bandwidth is 0.007, and tracking of the observed ramp is marginal at the higher-gain operating points. For a safety factor in the presence of the above ramp, it is recommended that, for stable operation, SSA conditions be chosen such that, at design point (at least for Compatibility Test Area (CTA 21) equipment):

$$\omega_L > 0.01 \text{ Hz} \tag{5}$$

To speculate on the source of the observed ramp is probably not valid; the ramp is there, its effects are part of each SSA installation, and it limits operating conditions. The probable third-order term, should it prove sizable, leaves the SSA with lock-drop potential under all conditions, except that time periods could be very long.

It is interesting to note that the synthesizer manufacturer's specification for the internal sweep calculator is:

$$\text{Frequency drift in 10 min} = \pm 50 \text{ Hz, maximum} \tag{6}$$

If this is divided by 10^4, as apparently occurs in the narrow-narrow SSA configuration, the result is a ramp of:

$$\frac{50}{600} \times 10^{-4} = 8.33 \times 10^{-6} \text{ Hz/sec maximum}$$

This is roughly twice the observed value.

VI. Part Two Outline

The ramp figures above are quite preliminary. To gain confidence in this parameter and its extensions, such as third and/or possibly higher-order terms, work under way on a much more sophisticated approach will be continued. This includes:

(1) Gathering of additional data sets exhibiting all modes.

(2) Coordinating parameter data through a series of loop-ramp cycles, using a generalized rms minimization program, to obtain ramp, rate, and higher-order data results with low variance, particularly during loop runs.

(3) In conjunction with (2), iterate phase vs S/N data through the S/N algorithm model to minimize the phase and time reduction errors.

(4) Determine the variation of the disturbing parameters between data sets, and their possible effect on data degradation under full in-lock conditions.

The expressions for the above steps are summarized in the Appendix.

VII. Summary

The SSA loop exhibits internal frequency instabilities; it has been estimated by ramp-period analysis at 25 times the maximum tracking rate in "narrow-narrow 8⅓" configuration, and only marginally in range if the bit rate is 33⅓. A third-order component may also be present.

Recommended minimum tracking bandwidth is 0.01 Hz, design point.

Part Two will extend these results and generalize operational limitations due to simple drift.

Table 1. Data set no. 1 phase conversion constants

Region	Mode	Sign	n	DBX	$\hat{\phi}$, deg
$T <$ First null	I	+	0	17.3	$0 < \hat{\phi} < 90$
	II	+	0	17.3	$0 < \hat{\phi} < 90$
First peak $> T >$ first null	I	−	1	17.3	$90 < \hat{\phi} < 157$
	II	−	1	14.8	$90 < \hat{\phi} < 180$
Second null $> T >$ first peak	I	+	0	17.3	$157 < \hat{\phi} < 90$
	II	+	1	14.8	$180 < \hat{\phi} < 270$
Second peak $> T >$ second null	I	+	0	17.3	$90 < \hat{\phi} < 0$
	II	−	2	16.0	$270 < \hat{\phi} < 360$
$T >$ second peak	I	−	0	17.3	$\hat{\phi} < 0$
	II	+	2	16.0	$\hat{\phi} > 360$

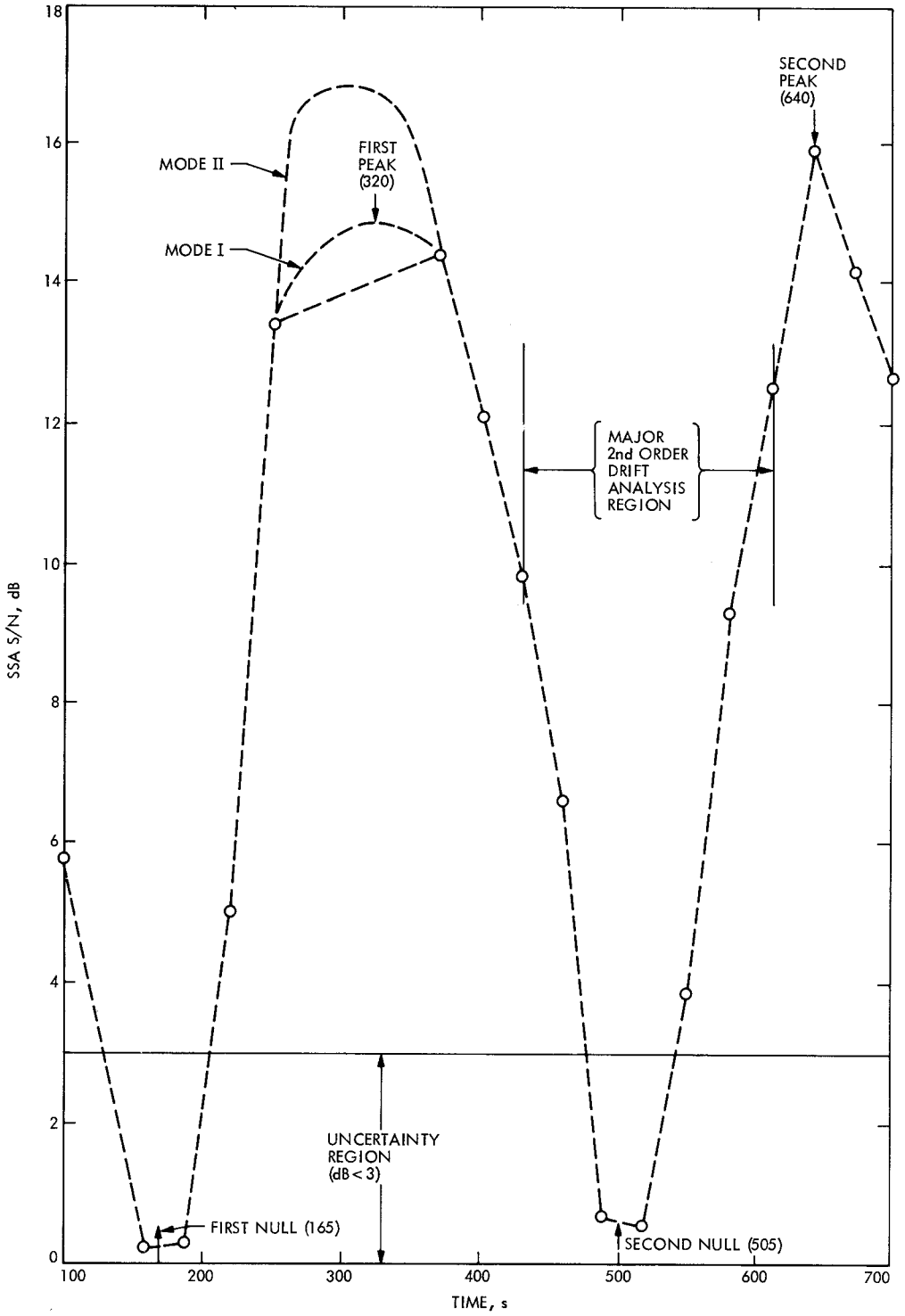

Fig. 1. SSA data set No. 1, CTA-21, March 1975. N-M bits/s raw data

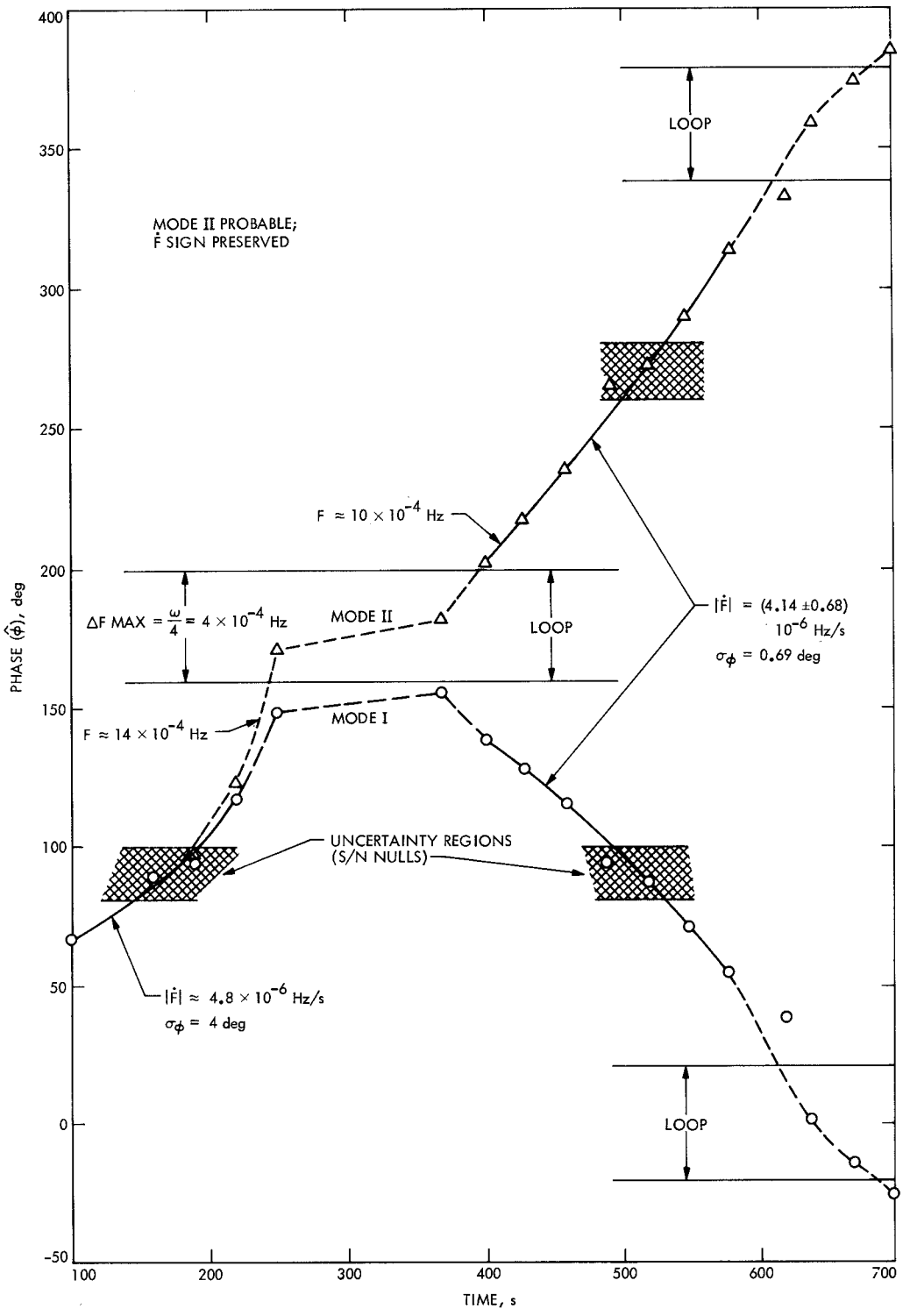

Fig. 2. SSA data set No. 1 phase estimate vs time. Two possible modes

Appendix

Program Models

Discussion begins at Part II of Fig. A-1. Let:

$$\phi'(t) = \begin{cases} F_1(t) \text{ loop} & \text{(exponential/trigonometric)} \\ F_2(t) \text{ ramp} & \text{(polynomial)} \end{cases}$$

Assume initial parameter estimates are available from ramp polynomial analysis. A "set" is one ramp-loop cycle. If phase noise is significant (ramp):

$$\phi''(t) = \sqrt{\frac{2}{\pi}}\,\sigma_\phi \exp\left[-\frac{1}{2}(\phi'(t)/\sigma_\phi)^2\right] + \phi'(t) \cdot \operatorname{erf}(\phi(t)/\sqrt{2}\,\sigma_\phi)$$

$$\sigma_\phi \approx \frac{1}{4} \cdot \sqrt{\frac{1}{R \cdot \operatorname{erf}(R)}}$$

R = system (max) S/N power ratio

If phase noise is insignificant:

$$\phi''(t) = \phi'(t)$$

For use in S/N reduction:

$$\phi(t) = |1 - 4 \cdot |\phi''(t) + \phi_m 1| 0 < \phi(t) < 1$$

ϕ_m effects covered above to obtain the phase noise mean. The S/N detector integral can be stated as (square-wave input):

$$y_i = \left| \int_{T_{0_i} - \Delta\tau}^{T_{0_i} - \Delta\tau + 2\phi(TC_i)\cdot\Delta\tau} [|V_i(t)| + n(t)]\,dt - \int_{T_{0_i} - \Delta\tau + 2\phi(TC_i)\cdot\Delta\tau}^{T_{0_i}} [|V_i(t)| - n(t)]\,dt \right|$$

TC_i = zero-crossing time; $\phi(TC_i)$ and TC_i require closure in $\phi'(t)$ and $\phi''(t)$.

T_{0_i} = completion time of the integral

= T_j at completion of sample set (final value)

$T_{0_i} = T_j - (N - i)\,\Delta\tau$

V_i = signal voltage @ $T_{0_i} - \Delta\tau$, reversing polarity @ TC_i, where phase value causes a step-function (assuming uncoded square-wave input)

$\Delta\tau$ = symbol period

N = number of symbols/samples: $\dfrac{(T_{j+1}) - T_j}{\Delta\tau}$

When $\phi(t)$ is variable, the moment solutions must necessarily carry a summation. The first two moments, taken over the S/N summation period, become extensions of well-known absolute value integrals:

$$X(T_j) = \epsilon\left\{\frac{1}{N}\sum_{i=1}^{N} Y_i\right\} = \frac{K}{N}\sum_{i=1}^{N}\left\{\sqrt{\frac{2}{\pi}} \cdot \exp - R[\phi(TC_i)]^2 + 2\sqrt{R}\,\phi(TC_i)\operatorname{erf}[\sqrt{R}\,\phi(TC_i)]\right\}$$

$$Y(T_j) = \epsilon\left\{\frac{1}{N}\sum_{i=1}(Y_i)^2\right\} = \frac{K^2}{N}\sum_{i=1}(2R \cdot \phi(TC_i) + 1)$$

$N\Delta\tau = TC$ = summation period (30 s)

$K = \sqrt{\dfrac{N_0 \cdot \Delta\tau}{2}}$, N_0 the noise spectral density

T_j = time of the readout time for the jth S/N measure

When S/N is high, as in this study (except for uncertainty around nulls), the two moments are sufficient. They combine to yield the S/N estimate:

$$(\widehat{S/N})_j = \frac{[X(T_j)]^2}{2\{Y(T_j) - \dfrac{n}{n-1} \cdot [X(T_j)]^2} = \frac{\bar{y}^2}{(\sigma^2 y)}$$

A given phase cannot be associated with this S/N. It represents summation over functions of the $\phi(TC_i)$, an entire section of the model curves:

$$\phi(T_j - \tau G) < \phi(S/N) < \phi(T_j)$$

For program use, three values were selected:

$$(\widehat{S/N})\,(T_j) \text{ represents} \begin{cases} \phi'(T_j - \tau G) \\ \phi'(T_j - \tau G/2) \\ \phi'(T_j) \end{cases}$$

Since S/N is predominantly an amplitude function, the difference between model results and data allowed original data estimates to be modified linearly:

$$\phi'_{\text{DATA}}(t) = \left[\frac{(S/N)_{\text{DATA}}}{(S/N)(T_j)}\right]^{1/2} \cdot \phi'(t)\, T_j - TG < t < T_j$$

ϕ'_{DATA}, three values, the replacement for former ϕ'. This provided data for phase iteration. The S/N to phase conversion above was the second and higher generation process; the original is covered in Part One.

To determine result quality, the S/N difference between data and model, scaled to the system S/N maximum ratio, was reduced to an rms value:

$$RMS^2 = \frac{1}{N}\sum_{i-1}^{N}\left[\frac{\sqrt{(S/N)_{i,\text{DATA}}} - \sqrt{(S/N)_{i,\text{MODEL}}}}{\sqrt{(S/N)_{\text{SYSTEM}}}}\right]^2$$

At each iteration, the "ramp" data was first subjected to a third-order fit and then, for each associated ramp-loop sequence, the entire parameter set was adjusted for the minimum mean-square condition by machine (small $\partial\Delta V$'s measured for each small "J parameter" at each point)

$$\Delta V_i = \frac{\sqrt{(S/N)_{i,\text{DATA}}} - \sqrt{(S/N)_{i,\text{MODEL}}}}{\sqrt{(S/N)_{\text{SYSTEM}}}}$$

$$E_i^2 = \left[\frac{\partial \Delta V_i}{\partial \phi_0}\cdot\Delta\phi_0 + \frac{\partial \Delta V_i}{\partial F_0}\cdot\Delta F_0 + \frac{\partial \Delta V_i}{\partial \dot{F}_0}\cdot\Delta\dot{F} + \frac{\partial \Delta V_i}{\partial \ddot{F}_0}\cdot\Delta\ddot{F}_0 + \frac{\partial \Delta V_i}{\partial \omega}\cdot\Delta\omega - \Delta V_i\right]^2$$

This leads to a system of simultaneous minimization equations from which parameter adjustments can be made. At completion, phases are readjusted and the process continued until no further reduction in RMS could be obtained.

Except on an exploratory basis, the above process has not yet been used. Additional data is required.

It remains to consolidate the program, set error measures, and bound applicability of results. This will be done in Part Two. Also, the following effect may be incorporated:

Phase Detector: Output Variation

In Part One, the effect of phase detector "flip-flop" at nulls was neglected, since the observed ramp magnitude far exceeded the maximum VCO ramp. However, the *frequency* changes are not as insignificant; the full "turnover" has the maximum final value:

$$|\Delta F_{\text{MAX}}| = 2 \cdot \zeta \cdot \omega \cdot |\Delta\phi| = 4 \cdot 10^{-4}\ \text{Hz}$$

This is a peak value at loop entry/exit; the actual value is noise dependent and nonlinear, being zero mean at the null.

Since actual observed frequencies fell between 10×10^{-4} and 18×10^{-4} Hz, this effect is significant in certain regions. The pending third-order model may "absorb" it, or, if it proves necessary, full phase detector noise theory in ramp regions may be applied.

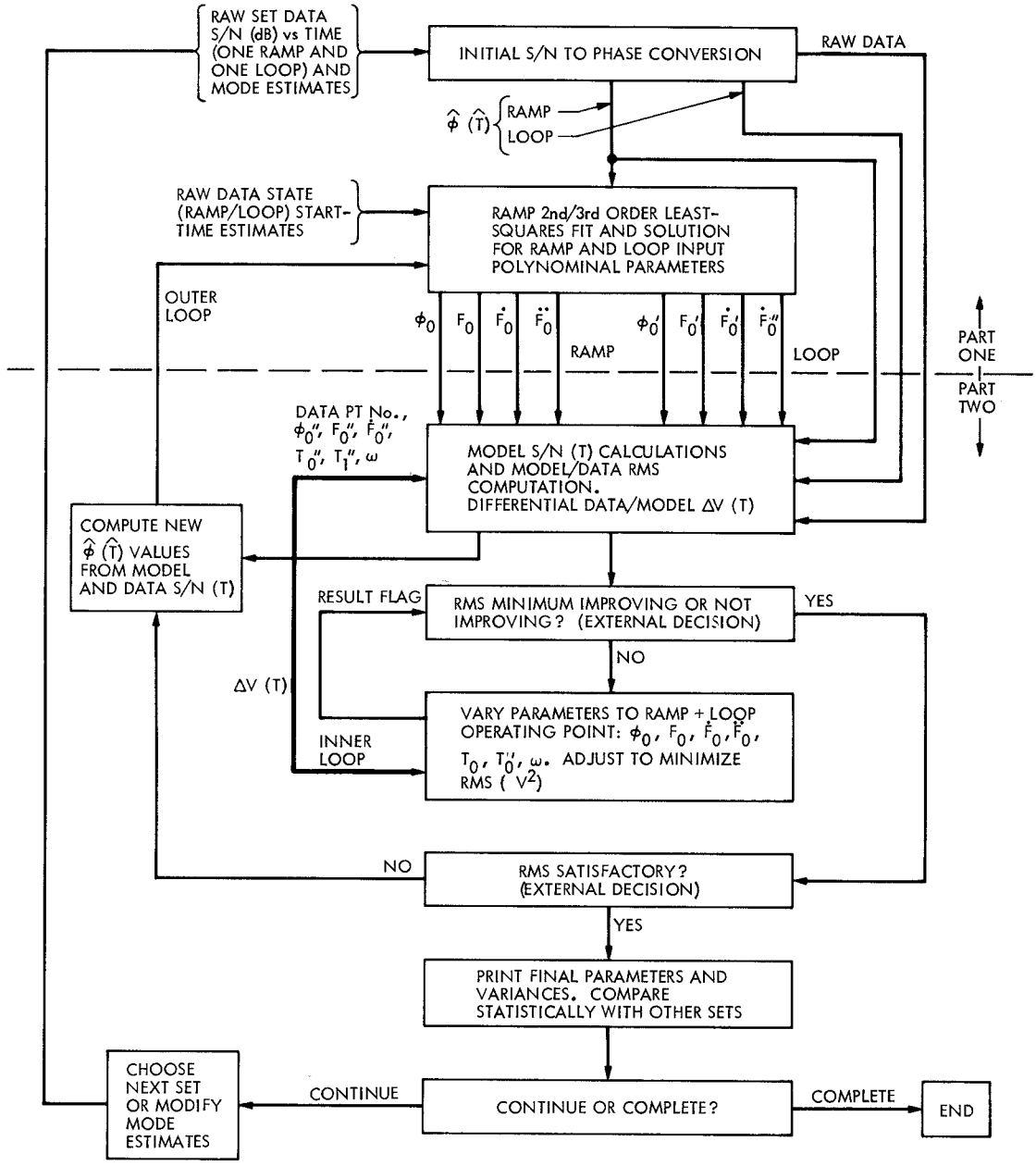

Fig. A-1. Machine data reduction plan, Part II SSA instability study